Immunity
Article

Tumor Necrosis Factor Signaling Mediates Resistance to Mycobacteria by Inhibiting Bacterial Growth and Macrophage Death

Hilary Clay,[1] Hannah E. Volkman,[1] and Lalita Ramakrishnan[2,*]
[1]Molecular and Cellular Biology Graduate Program, University of Washington, Seattle, WA 98195, USA
[2]Departments of Microbiology, Immunology, and Medicine, University of Washington, Seattle, WA 98195, USA
*Correspondence: lalitar@u.washington.edu
DOI 10.1016/j.immuni.2008.06.011

SUMMARY

Tumor necrosis factor (TNF), a key effector in controlling tuberculosis, is thought to exert protection by directing formation of granulomas, organized aggregates of macrophages and other immune cells. Loss of TNF signaling causes progression of tuberculosis in humans, and the increased mortality of *Mycobacterium tuberculosis*-infected mice is associated with disorganized necrotic granulomas, although the precise roles of TNF signaling preceding this endpoint remain undefined. We monitored transparent *Mycobacterium marinum*-infected zebrafish live to conduct a stepwise dissection of how TNF signaling operates in mycobacterial pathogenesis. We found that loss of TNF signaling caused increased mortality even when only innate immunity was operant. In the absence of TNF, intracellular bacterial growth and granuloma formation were accelerated and was followed by necrotic death of overladen macrophages and granuloma breakdown. Thus, TNF is not required for tuberculous granuloma formation, but maintains granuloma integrity indirectly by restricting mycobacterial growth within macrophages and preventing their necrosis.

INTRODUCTION

Pathogenic mycobacteria are highly adapted intracellular pathogens that can survive for indefinite periods of time within their hosts. Infection results in the recruitment of host macrophages to the bacteria, their phagocytosis, and the transit of infected macrophages into deeper tissues (Cosma et al., 2003; Dannenberg, 1993). There the infected macrophages recruit additional macrophages and other immune cells to form tightly aggregated immune structures called granulomas, pathological hallmarks of tuberculosis (Cosma et al., 2003; Dannenberg, 1993). In certain host species, areas within tuberculous granulomas undergo necrosis, referred to as caseation, so that mycobacteria may occupy both an intracellular and extracellular niche during the course of tuberculosis (Cosma et al., 2003).

Tumor necrosis factor (TNF) is one of the first effector molecules found to be essential in the host protective response against tuberculosis (Flynn et al., 1995). Mice deficient either in TNF or TNF receptor 1 have increased susceptibility to challenge with pathogenic mycobacteria (Bean et al., 1999; Flynn et al., 1995; Kaneko et al., 1999). The importance of TNF signaling in protection against human tuberculosis has become especially clear as a result of the increasing use of TNF-neutralizing drugs in treating a variety of immune and inflammatory conditions such as rheumatoid arthritis (Criscione and St Clair, 2002; Keane, 2005). Patients receiving TNF-neutralizing therapy have an increased rate of reactivation of latent tuberculosis (Gardam et al., 2003). Similarly, TNF is required to prevent active disease in mouse models of latent tuberculosis (Botha and Ryffel, 2003; Chakravarty et al., 2008; Mohan et al., 2001), suggesting it is required for the control of active as well as latent tuberculosis.

TNF can be produced by a variety of immune cells including macrophages, neutrophils, and T cells (Vassalli, 1992) and has pleiotropic effects in inflammation that affect cell activation and migration, apoptosis, and other biological processes (Locksley et al., 2001). Despite extensive investigation, the effects of the TNF pathway that play consequential roles in tuberculosis pathogenesis remain undefined. In vitro studies using cultured macrophages have implicated TNF in distinct and contradictory roles in mycobacterial pathogenesis, including induction of macrophage apoptosis that in turn leads to mycobacterial death (Fratazzi et al., 1999), activation of macrophage antimicrobial effectors to reduce mycobacterial numbers (Appelberg et al., 1994; Flesch and Kaufmann, 1990), or surprisingly, even enhancing mycobacterial growth (Engele et al., 2002). However, the in vivo studies that followed have led to the prevailing view that TNF is responsible for granuloma formation and maintenance, on the basis of the finding of disorganized granulomas after infection of TNF-deficient mice (Algood et al., 2005; Bean et al., 1999; Chakravarty et al., 2008; Flynn and Chan, 2001; Kindler et al., 1989; Roach et al., 2002; Stenger, 2005). This hypothesis is consistent with TNF's well-known role in orchestrating macrophage trafficking and leukocyte movement during inflammation (Kindler et al., 1989). The correlation of the protective role of TNF with the formation of granulomas, considered to be host-protective structures, is also consistent with the concept that tuberculous granulomas benefit the host by containing and restricting mycobacteria (Flynn and Chan, 2001; Lawn et al., 2002; Ulrichs and Kaufmann, 2006). This model is supported by the concomitance of poorly formed granulomas and

hypersusceptibility to infection that occur under various immunocompromising conditions in humans and mice (Flynn and Chan, 2001; Kaufmann, 2000; Lawn et al., 2002). More recently, studies of *Mycobacterium bovis*, BCG infection in TNF- and T cell-deficient mice suggested that at least in the context of this attenuated strain, TNF exerts its effects primarily by dampening overactive T cell responses and reducing granuloma and lung-tissue destruction, rather than acting during the innate immune phase of the response to mycobacterial infection (Zganiacz et al., 2004). Consistent with this anti-inflammatory role ascribed to TNF, other studies have suggested that in tuberculosis TNF deficiency mediates pathology and granuloma destruction that is independent of the increased bacterial numbers that are also found (Ehlers et al., 1999; Smith et al., 2002).

The accessibility and optical transparency of the developing zebrafish allows for a variety of unique experimental approaches to study pathogenesis, including vital microscopy, whole-mount in situ hybridization, and modified antisense oligonucleotides (morpholinos) for functional gene knockdowns (Trede et al., 2004). Zebrafish develop tuberculosis-like disease when infected with *Mycobacterium marinum*, a natural pathogen of ectotherms and the closest genetic relative of the *Mycobacterium tuberculosis* complex (http://www.sanger.ac.uk/Projects/M_marinum/) (Stinear et al., 2008). The virulence factors tested to date suggest that *M. marinum* and *M. tuberculosis* share virulence mechanisms and effectors (Cosma et al., 2006; Stamm et al., 2003; Tobin and Ramakrishnan, 2008; Volkman et al., 2004). Infection of adult zebrafish produces disease with hallmarks of active human tuberculosis, including caseation necrosis (Swaim et al., 2006). Adult zebrafish have a complex adaptive immune system akin to that of mammals (Traver et al., 2003), and infection with *M. marinum* is moderated by adaptive immunity similar to the case with mammalian tuberculosis (Swaim et al., 2006). Advantageously, zebrafish can be infected and monitored during early development when adaptive immunity has not yet developed (Trede et al., 2004), allowing for the dissection of the contribution of innate and adaptive immunity to infection (Clay et al., 2007; Davis et al., 2002). *M. marinum*-infected zebrafish embryos develop disease with essential features of adult tuberculosis, including granuloma formation, showing that the early steps of mycobacterial pathogenesis result from interactions of mycobacteria with the innate immune system (Davis et al., 2002). This model allows for the sequential visualization of infection in single animals (Clay et al., 2007; Cosma et al., 2006; Davis et al., 2002; Volkman et al., 2004).

Using the zebrafish-*M. marinum* model, we previously demonstrated that TNF is induced in macrophages very early in infection and that innate macrophages can restrict mycobacterial growth without input from the adaptive immune system (Clay et al., 2007). Here, we used morpholinos to ablate TNF signaling to reveal a substantial protective TNF effect that begins early and in the sole context of innate immunity in mycobacterial infection. We found that macrophage trafficking and granuloma formation were not dependent on TNF signaling. Rather, the absence of TNF signaling led to an increase in intracellular bacterial burdens accompanied by accelerated granuloma formation and the necrotic death of infected macrophages within well-formed granulomas. Granuloma necrosis then rendered the bacteria extracellular where their unrestricted growth continued to increase bacterial burdens. Thus, TNF mediates its primary protective effects in early infection by modulating bacterial growth and macrophage death.

RESULTS

Knockdown of TNF Receptor 1 Increased Susceptibility to *M. marinum* in the Context of Innate Immunity

The zebrafish genome encodes two putative TNF ligands with Zfin database identification numbers ZDB-GENE-050317-1 and ZDB-GENE-050601-2. Because of higher sequence homology and the upregulation of the latter of these during infection with *M. marinum* and other pathogens (Clay et al., 2007; Pressley et al., 2005; Rojo et al., 2007), this gene has been identified as the zebrafish TNF ortholog. Although fluorescent in situ hybridization reveals TNF expression in macrophages (Clay et al., 2007), infected Pu.1 morphant embryos lacking macrophages were found to express TNF by endpoint reverse transcriptase PCR, suggesting that other cell types also produce TNF in response to *M. marinum* infection (data not shown).

Two splice-blocking morpholinos (Draper et al., 2001) were designed against the TNF receptor 1 (TR1) ortholog (ZDB-GENE-040426-2252) in order to completely abolish TNF signaling, including any that may occur via the alternate TNF gene in the zebrafish genome (see Figure S1 available online). Injection of these morpholinos into fertilized eggs resulted in complete abrogation of native TR1 mRNA for 5 to 6 days postfertilization (dpf) with partial blocking thereafter for at least 10 dpf (Figure S1 and data not shown).

These TR1 morphant embryos survived similarly to control embryos even when raised under conventional conditions in the presence of their normal commensal flora (Figure 1A) and appeared morphologically normal throughout the observation period. The morphants cleared intravenously injected nonpathogenic *Escherichia coli* at rates similar to that of controls in a dose-dependent fashion. Both control and TR1 morphant embryos cleared one to ten CFU of *E. coli* within one day, ~50 CFU within two days, and ~100 CFU within three days of infection with no mortality of the embryos (data not shown).

Upon intravenous *M. marinum* infection, TR1 morphants succumbed to infection significantly more quickly than their control counterparts, reminiscent of the increased mortality of TNF-deficient mice infected with *M. tuberculosis* (Figure 1A) (Flynn et al., 1995). The TR1 morphants had a hazard ratio for death of 5.7 over the 12 day observation period ($p < 0.0001$, Kaplan Meier method with log-rank test) and a median time to death of 9 days versus 12 days. Increased mortality of the embryos was also associated with up to ten-fold greater bacterial burdens in the TR1 morphants as compared to control embryos in the first six days (Figures 1B and 1C), comparable to the increased bacterial numbers seen in TNF-deficient mice early in infection (Flynn et al., 1995; Stenger, 2005). These results show that TNF signaling is important for the modulation of mycobacterial infection from its early stages and does not require adaptive immunity for protective effects in vivo.

TNF Signaling Is Not Required for Macrophage Migration in Response to Infection

Having confirmed that TNF deficiency in zebrafish embryos leads to the endpoint phenotypes of increased mortality and

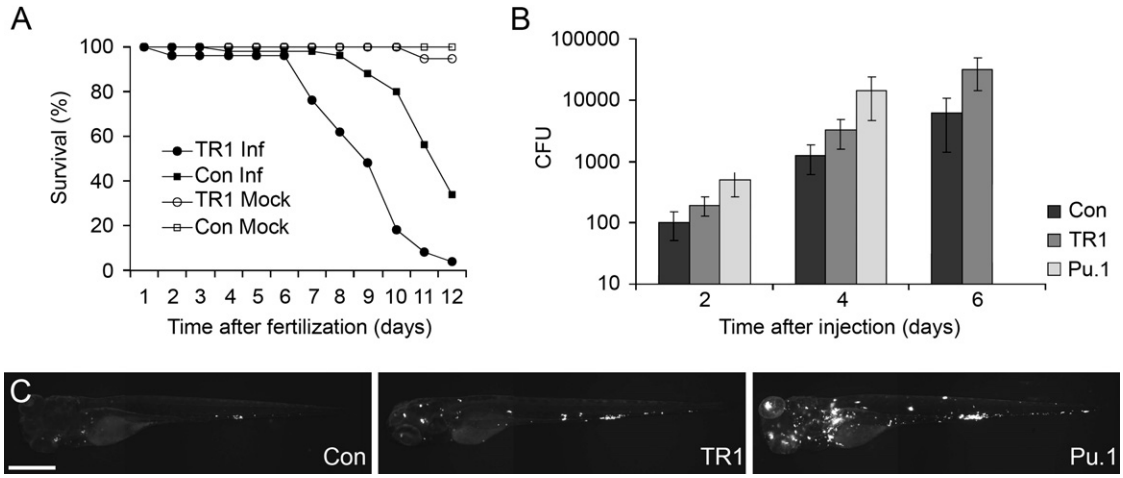

Figure 1. TR1 Morphant Embryos Are More Susceptible to Mycobacterial Infection

(A) Control (Con) and TR1 morphant embryos were either mock injected (n = 30 each) or infected with 108 ± 11 colony forming units (CFU) of *M. marinum* on 1 dpf (n = 50 each). Data are plotted as the percentage of surviving embryos on each day. TR1 morphant embryos are significantly more susceptible to infection with *M. marinum* than controls (Hazard ratio 5.7, $p < 0.0001$, Kaplan Meier method with log-rank [Mantel-Cox] test). Survival was not statistically different between mock-injected TR1 and control embryos.

(B) Mean bacterial loads per embryo for control (Con), TR1, and Pu.1 morphant embryos at 2, 4, and 6 days post injection (dpi) with 70 ± 13 CFU. $p < 0.0001$ by one-way ANOVA. Data for Pu.1 embryos are only available for 2 and 4 dpi because of mortality. Error bars represent standard deviation from the mean. All morphant bacterial loads are significantly different from one another ($p < 0.05$) at each individual time points (control versus TR1, control versus Pu.1, and TR1 versus Pu.1) by Student's unpaired t test.

(C) Representative pictures of control, TR1, and Pu.1 morphant embryos at 4 dpi with fluorescence representing bacterial load. The scale bar represents 500 μm.

bacterial growth seen in TNF deficiency in adult mammals, we set out to determine the specific steps of mycobacterial pathogenesis at which TNF acts by taking advantage of the transparency of the zebrafish. Because TNF signaling has been implicated in macrophage activation and migration (Vassalli, 1992), we first sought to determine whether mycobacteria could recruit phagocytes across epithelial barriers in the absence of TNF signaling by assessing macrophage recruitment to bacteria introduced into the hindbrain ventricle (Davis et al., 2002; Herbomel et al., 1999). The hindbrain ventricle is a neuroepithelial-lined cavity that is structurally separated from the circulatory system and the yolk mesenchyme in which macrophages arise during early development; this cavity is normally devoid of macrophages in the first 24 hr after fertilization (Davis et al., 2002; Herbomel et al., 2001). We had previously demonstrated that phagocytes, readily identified by their morphology with differential interference contrast (DIC) microscopy, are specifically recruited to this cavity upon injection of mycobacteria, but not like-sized latex particles (Clay et al., 2007; Davis et al., 2002). Similar numbers of phagocytes were recruited to the hindbrain ventricle after injection of *M. marinum* into TR1 morphant and control embryos (6 ± 1 macrophages in control and 6 ± 3 macrophages in TR1 morphant embryos) (Figure S2). Macrophages phagocytosed the bacteria and migrated back into tissues normally in the TR1 morphants so that within 24 hr of hindbrain ventricle or caudal vein injection, the majority of bacteria had reached deeper tissues within macrophages (Figure 1C and data not shown). These results suggest that TNF signaling is not required for phagocyte trafficking across epithelial and endothelial barriers; macrophages are competent to respond and traffic to peripheral sites of infecting mycobacteria in the absence of TNF signaling.

Granuloma Formation Is Accelerated in the Absence of TNF Signaling

The developing zebrafish is an ideal host in which to monitor early granuloma formation because of our ability to follow infected macrophages in individual animals over time (Davis et al., 2002; Volkman et al., 2004). Infection of developing zebrafish leads to the formation of macrophage aggregates that are easily identifiable by DIC microscopy and that have characteristic pathological hallmarks of adult tuberculous granulomas, including epithelioid transformation of macrophages (Davis et al., 2002). In addition, several mycobacterial genes that are induced in granulomas of adult animals (granuloma-activated genes [*gag*s]) are also induced rapidly and selectively upon macrophage aggregation into granulomas in the developing zebrafish (Davis et al., 2002). Hereafter, we will refer to the early granulomas in the developing zebrafish simply as granulomas.

In contrast with our expectation that TNF directs macrophage trafficking into granulomas, DIC microscopy revealed an abundance of granulomas in *M. marinum*-infected TR1 morphant embryos (Figures 1C and 2A). To investigate this surprising result further, we assayed granuloma formation by several methods. We first used the fluorescence of *M. marinum*-expressing transcriptional fusions of GFP to *gag*7 (RecC) and *gag*3.13 (homolog of *M. tuberculosis* Rv0133, a putative *N*-acetyltransferase) as sensitive indicators of granuloma formation (Davis et al., 2002) in the presence and absence of TNF signaling. Control and TR1 morphant embryos were infected with *gag*7::*gfp* and *gag*3.13::*gfp* *M. marinum*, and the percentage of embryos with fluorescent bacteria was assessed after 4 days. A higher proportion of TR1 morphant embryos had formed *gag*-positive granulomas in comparison to control embryos at 4 dpi (Figures 2A and 2B) corroborating our impression from our initial qualitative DIC microscopy.

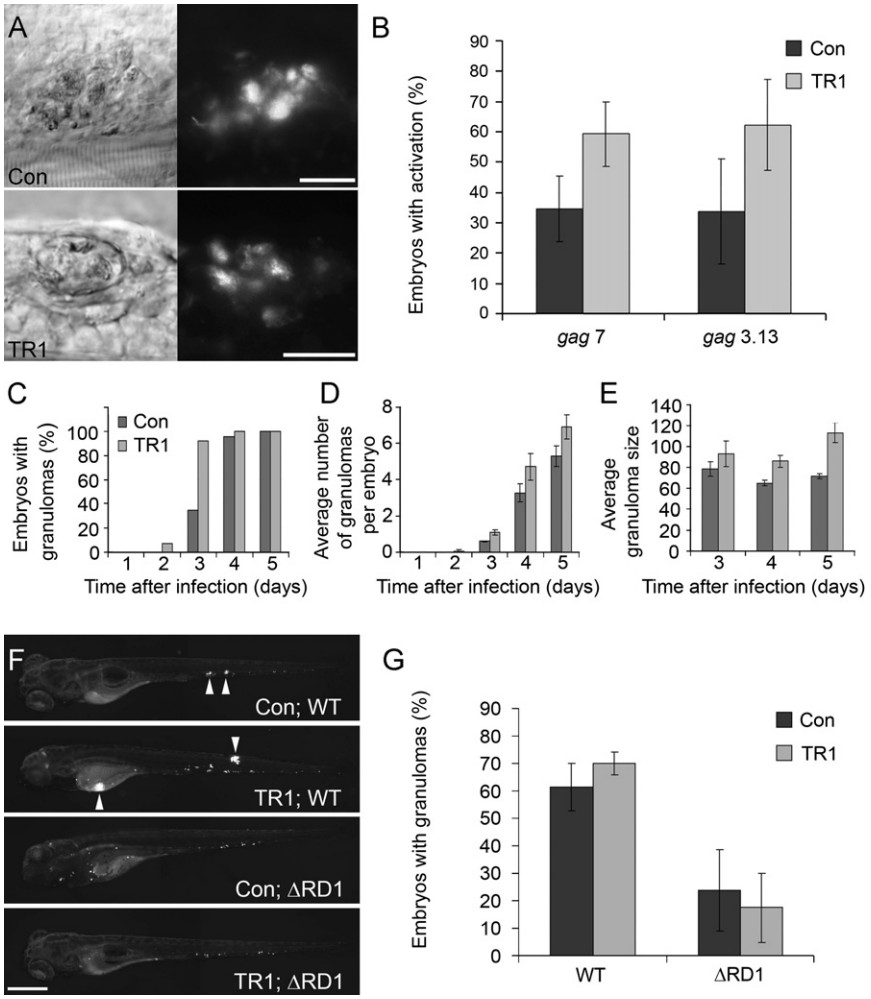

Figure 2. Granulomas Form More Quickly in the Absence of TNF Signaling

(A) DIC (left) and fluorescence (right) images of granuloma. Activated genes (*gag*3.13) in granulomas in both control and morphant embryos are shown as percentage of embryos with activation of fluorescent reporters ± the standard deviation of the mean. Scale bars represent 25 μm.

(B) Three pools of ~30 embryos were injected with 56 ± 18 CFU of *gag*7, and four pools of ~30 embryos were injected with 64 ± 17 CFU of *gag*3.13. All groups were scored at 4 dpi for induction of *gag*s as indicated by fluorescent activity. The average percentage of embryos with *gag* induction is plotted ± standard deviation of the mean. Averages for both *gag*7 and *gag*3.13 are significantly different between controls and morphants ($p < 0.05$, Student's unpaired t test).

(C–E) 23 Control and 14 TR1 morphant embryos were injected with 89 ± 4 CFU and followed sequentially for 5 dpi and monitored for granuloma formation and size. All dark bars represent control morphant data; light bars represent TR1 morphant data. Data are plotted as average ± standard error of the mean. (C) shows the percentage of embryos with at least one granuloma over time. TR1 morphant embryos have significantly more granulomas at 3 dpi ($p < 0.01$) as analyzed by Fisher's exact test of a contingency table. (D) shows the average number of granulomas identified by DIC and fluorescent microscopy over time. (E) shows that TR1 morphant granulomas are significantly larger than control granulomas ($p < 0.05$ at 3 dpi, $p < 0.0001$ at 4 and 5 dpi by Student's unpaired t test, n = 14; control and 14 TR1 granulomas at 3 dpi, 75 control and 53 TR1 granulomas at 4 dpi, and 113 control and 72 granulomas at 5 dpi). The y axis represents granuloma diameter in μm.

(F and G) Pools of 20 embryos were injected with 27 ± 6 wild-type (WT) and 51 ± 13 ΔRD1 *M. marinum* and assayed by microscopy at 4 dpi for granuloma formation. (F) shows representative images of control and TR1 morphant embryos. Arrowheads indicate granulomas. The scale bar represents 200 μm. As shown in (G), the average percentage of embryos with granulomas is plotted ± standard deviation of the mean over four biological replicates. The percentage of embryos with granulomas is significantly higher when injected with WT ($p < 0.01$ for Con; WT versus Con; ΔRD1 and $p < 0.001$ for TR1; WT versus TR1; ΔRD1 by Student's unpaired t test).

In order to better characterize the increase in granuloma formation seen in the absence of TNF signaling, we monitored granuloma formation and size over time by DIC and fluorescence microscopy in control and TR1 morphant embryos. TR1 morphant embryos formed granulomas more quickly than controls (Figure 2C). At all time points, TR1 morphants had more granulomas than control embryos, although this difference was not statistically significant (Figure 2D). Moreover, the average size of granulomas was significantly larger in TR1 morphant embryos at all time points, suggesting a persistent acceleration in granuloma growth beyond the initial aggregation event (Figure 2E).

In the face of the widely held view that TNF signaling mediates granuloma formation (Algood et al., 2005; Flynn and Chan, 2001; Kindler et al., 1989; Lin et al., 2007; Roach et al., 2002), we wanted to investigate further our finding that granuloma formation was not impaired but rather enhanced in the absence of TNF. Although the simplest explanation of this finding is that TNF does not mediate granuloma formation, we considered the alternative possibility that TNF signaling does mediate granuloma formation but that this phenotype is obscured by a distinct mechanism of granuloma formation that becomes operant in its absence. To investigate this question, we used the *M. marinum* mutant that is deficient in the ESX-1 (RD1) secretion locus and that produces infection with delayed and defective granulomas (Volkman et al., 2004). We compared granuloma formation by DIC and fluorescent microscopy, assaying for discrete foci of tightly packed infected macrophage aggregates in control and TR1 morphant embryos infected with wild-type (WT) and ΔRD1 bacteria at 4 dpi. The aggregation defect of ΔRD1 was maintained in the presence and absence of TNF signaling (Figures 2F and 2G). These data showed that granuloma formation proceeds via a mycobacterial RD1-dependent fashion regardless of whether TNF signaling is present. Therefore, the abrogation of TNF signaling does not uncover a distinct pathway of accelerated granuloma formation. Rather, these findings suggest that granulomas form in the course of normal infection by a pathway that is independent of TNF signaling. In summary, these data show that rather than preventing macrophage aggregation into

granulomas, the loss of TNF signaling leads to an accelerated kinetics of granuloma formation and expansion. Notably, despite the absence of granuloma formation, we found some overall increase in bacterial burdens in the TR1 morphants during ΔRD1 infection (data not shown), suggesting that TNF signaling exerts its protective effect earlier than and independently of granuloma formation. This finding is also consistent with previous studies showing that TNF signaling exerts its protective effect in mice infected with *M. bovis* BCG that lacks RD1 (Kindler et al., 1989; Zganiacz et al., 2004).

TNF Signaling Exerts Protection In Vivo via Its Macrophage Mycobactericidal Activity

We have previously demonstrated that macrophages restrict mycobacterial growth from very early on during infection accompanied by TNF induction in infected macrophages (Clay et al., 2007). The increased total bacterial burdens found in TR1 morphant embryos from very early in infection even prior to granuloma formation further suggest that TNF signaling exerts a protective effect in vivo by mediating macrophage microbicidal activities (Figure 1B). This early increase in bacterial numbers in individual macrophages could then lead to accelerated granuloma formation in TR1 morphant embryos. This model is supported by our finding that higher infecting inocula lead to more rapid granuloma formation (data not shown).

We sought to determine whether TNF signaling mediated macrophage microbicidal activities by enumerating the numbers of bacteria in individual macrophages during infection (Cosma et al., 2006). However, we were unable to make this determination with wild-type bacteria because even low-dose inocula induced accelerated granuloma formation in the TR1 morphant (Figure 2C), with selective recruitment of highly infected macrophages into granulomas in which they could not be scored, leaving insufficient numbers of highly infected individually infected macrophages available for analysis. To circumvent the rapid kinetics of granuloma formation with wild-type bacteria in the TR1 morphant, we took advantage of the attenuated *M. marinum* Erp mutant that is defective for growth in individual macrophages. The intramacrophage growth defect of the Erp mutant is responsible for its attenuation phenotype, which is rescued in Pu.1 morphant embryos lacking macrophages (Clay et al., 2007). Secondary to its macrophage growth defect, the Erp mutant also has reduced granuloma formation (data not shown). Therefore, we reasoned that assessing the phenotype of the Erp mutant in TR1 morphant embryos would isolate TNF-signaling-mediated macrophage mycobactericidal effects from its other possible protective effects on infection. First, we found overall increased growth of the Erp mutant bacteria in the TR1 morphants as evidenced by increased bacterial burdens by fluorescence microscopy (Figure 3A). Increased bacterial burdens were associated with increased mortality of the TR1 morphant embryos as compared to controls (mean time to death 9.6 versus 10.8 days, $p < 0.01$ by Student's unpaired t test). Next, we scored the bacterial burdens of individual infected macrophages in the embryos as previously described (Cosma et al., 2006). As predicted, the slower growth of the Erp mutant allowed for individual macrophage burdens to be assessed at a time point before all the macrophages had been recruited into granulomas, thereby allowing for a higher number of infected macrophages to be scored for bacterial burdens; such scoring is not possible after macrophages are tightly aggregated. TR1 morphant embryos infected with Erp mutant bacteria had a significantly higher percentage of macrophages with high intracellular bacterial burdens (scored as more than ten bacteria per macrophage versus low intracellular bacterial burdens as ten or fewer bacteria per macrophage) ($p < 0.05$, Student's unpaired t test) compared to control embryos (Figures 3B–3D). These results suggest that TNF signaling exerts a protective influence by restricting intracellular mycobacterial growth in vivo. On the basis of our finding that wild-type bacterial burdens in the TR1 morphants are significantly higher than in controls, but not as high as those in the Pu.1 morphants (Figures 1B and 1C), we conclude that TNF signaling is upstream of part, but not all, of macrophage effector mechanisms for combating mycobacterial growth in individual macrophages by enabling their microbicidal (or bacteriostatic) activity.

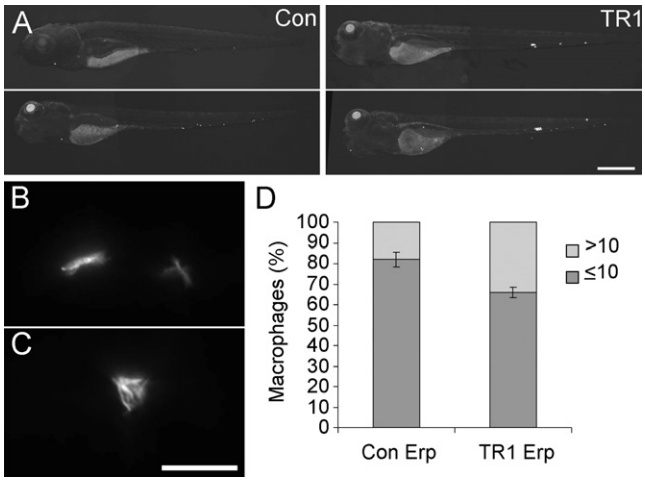

Figure 3. Growth of Erp Mutant Bacteria Is Partially Restored in TR1 Morphant Embryos

(A) Representative fluorescence images for control (Con) and TR1 morphant fish infected with 55 ± 7 CFU of Erp mutant (Erp) *M. marinum* at 4 dpi. The scale bar represents 500 μm.

(B–D) A total of 50 individual macrophages were scored for multiplicity of infection (MOI) as either containing (B) 10 or less bacteria or (C) more than 10 bacteria at 3 dpi during infection with 55 ± 7 CFU of Erp mutant bacteria. The scale bar represents 25 μm. As shown in (D), the percentage of macrophages (out of 50) scored as either having more than ten, or ten or less bacteria per macrophage ± standard deviation of the mean in TR1 morphant versus control embryos. TR1 morphants had a significantly greater percentage of macrophages with more than ten bacteria as compared to controls ($p < 0.05$, Student's unpaired t test).

The effector molecule most widely ascribed to combating mycobacterial growth in macrophages is the reactive intermediate nitric oxide, made by the inducible nitric oxide synthase (iNOS) (Kwon, 1997). In order to determine whether iNOS is induced during infection of zebrafish embryos with *M. marinum*, we used fluorescent antibody detection of iNOS protein and co-localized infected cells with iNOS antibody staining. Both control and TR1 morphant embryos displayed iNOS staining that co-localized with a subset of infected macrophages (Figure S3). We were unable to determine any differences in staining between control and TR1 morphant embryos, suggesting that TNF signaling is not required for iNOS expression in our system, consistent

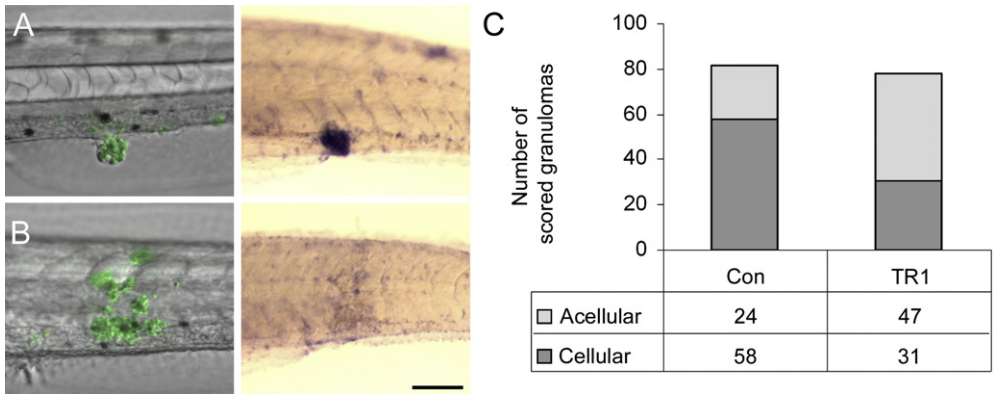

Figure 4. TR1 Morphant Embryos Have Significantly More Acellular Granulomas than Controls

(A and B) Differential interference contrast overlay with fluorescence (left) of infected embryos then labeled with in situ hybridization for the macrophage marker *fms* (right). Green indicates *M. marinum* in fluorescent overlays. Purple staining of hybridized embryos indicates expression of the macrophage marker *fms*. (A) shows an example of a cellular granuloma in a control embryo before and after in situ hybridization indicating bacteria within aggregated macrophages. (B) shows an acellular granuloma example in a TR1 morphant embryo indicating bacteria found primarily outside of macrophages.

(C) The number of granulomas scored as either cellular or acellular in TR1 morphant versus control embryos. TR1 morphant granulomas were twice as likely to contain one-third or fewer *fms*-positive cells than to WT granulomas ($p < 0.0001$) as analyzed by Fisher's exact test of a contingency table. Embryos were 7 dpf and infected with 267 ± 28 CFU.

with previous reports in other systems (Bean et al., 1999; Bekker et al., 2000; Ehlers et al., 1999).

Nonapoptotic Death of Granuloma Macrophages Is Increased in the Absence of TNF

Our sequential imaging of live infected fish showed that although granulomas formed rapidly and appeared normal at first in the TR1 morphant embryos (Figure 2A), a combination of fluorescence and DIC microscopy revealed that they began to appear larger and more acellular than control granulomas soon after they had formed. To confirm this observation, we developed a quantitative assay to assess the cellularity of granulomas in control versus TR1 morphants using colorimetric whole-mount in situ hybridization (WISH) analysis labeling the *fms* gene, a macrophage-specific marker encoding the macrophage colony-stimulating factor receptor (M-CSFR) (Clay and Ramakrishnan, 2005; Parichy et al., 2000). Only live macrophages will express *fms* mRNA and therefore hybridize to the probe (Figures 4A and 4B). WISH analysis was performed on control and TR1 morphant embryos 6 dpi. We scored granulomas by using a blinded visual assay with DIC microscopy to identify bacterial masses as being mostly cellular (greater than one-third of the granuloma mass hybridizing to the *fms* probe) (Figure 4A) or acellular (one-third or less of the granuloma mass hybridizing to the *fms* probe) (Figure 4B). Scoring of all of the individual granulomas from the two groups showed that twice as many of the TR1 morphant granulomas were acellular as compared to granulomas from control embryos (Figure 4C). Although *fms* staining did not appear different between uninfected TR1 and control morphant embryos, there did appear to be an overall reduction in *fms*-positive cells in infected TR1 morphants (data not shown), suggesting that the accelerated macrophage death resulting from the loss of TNF signaling leads to their overall depletion.

TNF has been shown to modulate cell death in inflammation by both pro- and antiapoptotic effects, and in vitro studies have suggested that TNF mediates apoptosis of *Mycobacterium*-infected macrophages that in turn results in death of the resident bacteria (Fratazzi et al., 1999; Stenger, 2005). Because the TR1 morphants had increased cell death associated with exuberant bacterial growth, we wondered whether it was due to a reduction in apoptosis caused by the absence of TNF signaling that channels infected cells into a default pathway of necrotic death. Necrosis of infected cells, in contrast to apoptotic death, is postulated to allow the bacteria to survive (Fratazzi et al., 1999). We have previously shown that some infected macrophages within granulomas undergo apoptosis as indicated by the terminal deoxynucleotidyl transferase-mediated deoxyuridine triphosphate nick end labeling (TUNEL) assay that labels double-strand DNA breaks (Volkman et al., 2004). We found that several of these TUNEL-positive macrophages express TNF as judged by dual fluorescent labeling of whole embryos with in situ hybridization for TNF expression and TUNEL labeling for apoptotic cells (Clay and Ramakrishnan, 2005) (Figures 5A–5D). This finding suggests that the TNF pathway could be modulating the apoptosis that occurs in granuloma macrophages. However we found no difference in the number of TUNEL-positive cells in like-sized granulomas of control and TR1 morphant embryos (Figure 5E). In contrast, we found the expected reduction in TUNEL-positive cells in granulomas that formed as a result of RD1-deficient *M. marinum* (ΔRD1) infection (Figure 5E) (Volkman et al., 2004). Next, we scored granulomas for either the presence or absence of TUNEL-positive cells and compared TR1 morphant and control embryos for the percentage of total granulomas that had at least one TUNEL-positive cell and again found no difference between the two groups (Figure 5F). With the recognition that some forms of apoptosis do not lead to detectable double-stranded DNA breaks (Huerta et al., 2007), these data suggest that TNF signaling does not modulate apoptotic macrophage death within granulomas. Furthermore, the increased cell death occurring in the absence of TNF signaling as evidenced by the acellular granulomas is independent of changes in TUNEL-positive apoptotic cell death.

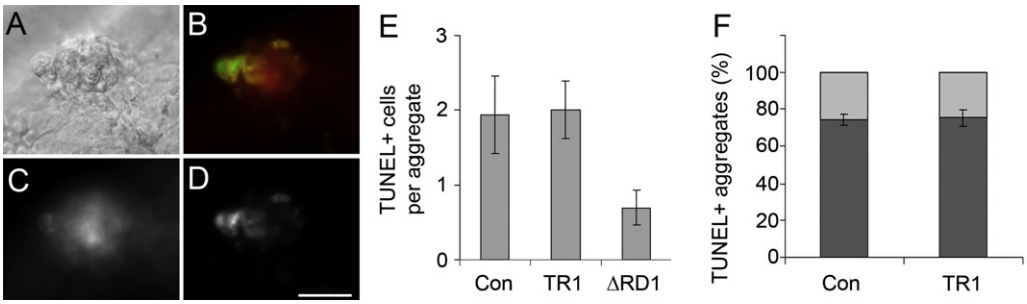

Figure 5. TNF Signaling Does Not Influence the Rate of Apoptosis of Infected Cells

DIC and fluorescent imaging of a granuloma are shown in (A) and (B)–(D), respectively. (B) shows colocalization of TNF expression (red) and TUNEL-labeled double-strand DNA breaks (green). Individual fluorescence channels for (C) TNF expression and (D) TUNEL-labeling are shown. The scale bar represents 50 μm. (E) shows the number of TUNEL-positive cells per granuloma ± standard deviation of the mean. The average number of TUNEL-positive cells within granulomas in 4 dpi embryos is unchanged between control (n = 16 granulomas) and TR1 morphant embryos (n = 20). Infection of control embryos with RD1-deficient bacteria (ΔRD1) is used as a control (n = 20). The number of TUNEL-positive cells in ΔRD1 granulomas is significantly less than control and TR1 morphant granulomas with wild-type bacteria ($p < 0.05$ by Student's unpaired t test for both comparisons). Granulomas were selected to be between 40 and 50 μm in diameter to normalize for total cell number. (F) shows the percentage of TUNEL-positive granulomas between control and TR1 morphant 4 dpi embryos ± standard error of the mean. Three separate experiments of pools of 20–40 granulomas were scored per condition and plotted as number of granulomas with TUNEL-positive cells over total granuloma number. Error bars represent standard error of the mean.

Extracellular Corded Mycobacteria Accumulate in the TR1 Morphants Leading to Accelerated Bacterial Growth and Spread

On imaging live embryos, we had found that concomitant with the loss of granuloma cellularity, the mycobacteria took on a corded appearance. Cording morphology, in which the bacteria are intertwined into serpentine rope-like structures (Koch, 1882), is a distinctive feature of *M. tuberculosis* grown in culture (Darzins and Fahr, 1956; Dubos and Pierce, 1956; Middlebrook et al., 1947). In *M. tuberculosis*, genetic mutations that abolish cording in vitro also result in reduced virulence (Bhatt et al., 2007; Glickman et al., 2000). However, although cording in vitro is tightly correlated to virulence, this phenotype has not been observed in vivo previously. In this light, we were first struck by the appearance of corded bacteria in the Pu.1 morphants (Clay et al., 2007) in which the bacteria are always extracellular (Figure 6A). In contrast, bacteria within macrophages do not exhibit this phenotype, suggesting that cording is a property of extracellular bacteria regardless of whether they are in vitro or in vivo (Figure 6B). Although not all extracellular bacteria demonstrate a cording phenotype, it serves as a conservative estimate of whether bacteria are growing extracellularly in vivo. We found that the percentage of embryos with corded bacteria was significantly greater in TR1 morphants than in control embryos from very early in infection (Figures 6C–6F). These results correlate with our findings of increased macrophage death in the absence of TNF signaling. Taken together, these data indicate that the absence of TNF signaling leads to increased macrophage death and necrotic breakdown of granulomas with resultant exuberant growth of extracellular mycobacteria. Notably, corded bacteria were not always restricted to the acellular granulomas. Individual clumps of corded bacteria were found that probably represent those released from a single dead macrophage (Figure 6E). This result suggests that TNF-pathway deficiency produces accelerated death of both individual and granuloma macrophages with release of extracellular bacteria.

To further dissect the pathway of the accelerated cell death occurring in the absence of TNF, we again used the *M. marinum* ESX-1(RD1) mutant. Infection of macrophages with the ESX-1(RD1) virulence locus in vitro produces increased cell death (Guinn et al., 2004; Hsu et al., 2003; Kaku et al., 2007). In the zebrafish, infection with ΔRD1 *M. marinum* results in fewer granulomas that contain TUNEL-positive cells (Volkman et al., 2004). In order to test whether bacterial RD1 is required for the increased macrophage cell death seen in the absence of TNF signaling, we infected control and TR1 morphant embryos with ΔRD1 and looked for the presence of cording bacteria. Despite the fact that ΔRD1 *M. marinum* infection remains partially attenuated in TR1 morphant embryos presumably because of their deficiency in forming granulomas (Figures 2F and 2G), infection of these morphants with higher doses of this attenuated strain revealed increased levels of cording bacteria in TR1 morphant embryos (Figure 7A). Consistent with the formation of poor granulomas, the majority of corded bacterial masses were smaller than those found during wild-type infection (compare Figures 7B and 7C to Figure 6D). This finding corroborated our observations with wild-type bacteria that individual macrophages with accelerated necrosis could be found outside of granulomas (Figure 6E). In wild-type infection, the accelerated formation of granulomas makes it more likely that macropahge necrosis occurs within granulomas. However, it is clear from these experiments that granuloma formation is not a prerequisite for macrophage necrosis. Taken together, these data indicate that increased cell death resulting from the lack of TNF signaling is not dependent on the ΔRD1 virulence locus or granuloma formation.

Additionally, time-lapse microscopy revealed several individual infected dead macrophages and even demonstrated that a single dead macrophage may provide a means for dissemination of infection (Figure S4 and Movie S1). In this example, a single infected macrophage in a TR1 morphant embryo is phagocytosed by two separate uninfected macrophages, indicating that the death of single infected host cells is capable of spreading bacteria to multiple uninfected macrophages. Thus, infected macrophage cell death could accelerate infection both by giving rise to extracellular bacteria as well as spreading infection to new macrophages. The ability of bacteria to remain extracellular in

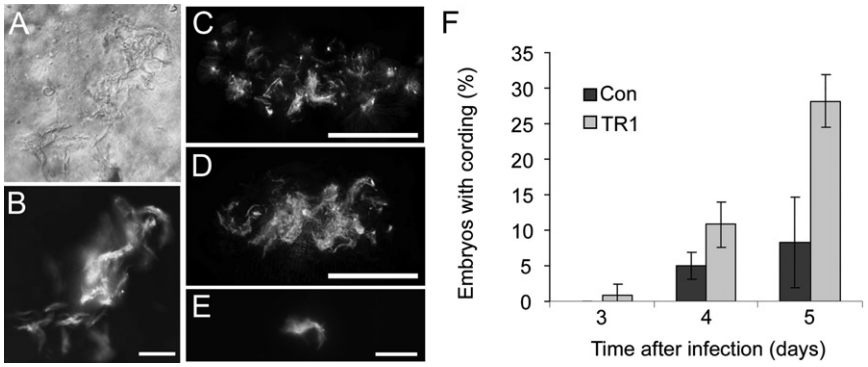

Figure 6. TR1 Morphant Embryos Are More Likely to Have Extracellular Bacteria as Indicated by Cording

DIC (A) and fluorescence (B–E) imaging of bacteria in vivo. As shown in (A) and (B), extracellular bacteria in Pu.1 morphant embryos without macrophages display the cording phenotype. The scale bar represents 25 μm. As shown in (C) and (D), flattened 3D Z stacks of control (C) and TR1 morphant (D) granulomas demonstrate cording in TR1 morphant embryos. Scale bars represent 50 μm. (E) shows cording after what appears to be breakdown of an individual infected macrophage in infected TR1 morphant embryo. The scale bar represents 25 μm. As shown in (F), four pools of 30 embryos were injected with 18 ± 5 CFU and scored daily for the presence of extracellular bacteria as indicated by cording and plotted as the percentage of embryos with cording ± the standard deviation. TR1 morphant embryos had significantly higher percentages of embryos with cording at all time points by Student's unpaired t test ($p < 0.05$ for 3 and 4 dpi, $p < 0.01$ for 5 dpi).

later stages of infection probably reflects a saturation effect in which uninfected macrophages available for rephagocytosis of extracellular bacteria are unable to keep up with the rate of bacterial growth and infected macrophage death.

DISCUSSION

Our detailed stepwise dissection of the consequences of TNF receptor loss to mycobacterial pathogenesis shows that an accelerated increase in bacterial numbers occurs from the very early stages of infection. Our prior work had demonstrated that innate macrophages are capable of limiting mycobacterial growth to a considerable extent and that TNF is induced in infected macrophages within 24 hr after infection (Clay et al., 2007). The finding that TR1 morphant embryos have an accelerated bacterial burden during this early phase of infection suggests that the TNF pathway plays a role in this early mycobacterial-growth restriction by macrophages. In support of this conclusion, we find that the specific macrophage growth defect of a mycobacterial mutant is partially rescued during infection of TNF-deficient embryos. Our finding that TNF is protective in early tuberculosis confirms experimental infection data in adult mammalian infection (Stenger, 2005) but is a formal demonstration that TNF signaling can exert its protective effects in vivo in the absence of adaptive immunity. By demonstrating that a key host protective determinant can exert its effects in the context of innate immunity alone, these results add to the growing appreciation for a substantial role for innate immunity as an autonomous mediator of tuberculosis control aside from serving as the effector arm of adaptive immunity (Berrington and Hawn, 2007; Clay et al., 2007; Pan et al., 2005; Tosh et al., 2006; van Crevel et al., 2002).

Consistent with other experimental models of mycobacterial infection, we find that loss of TNF signaling leads to an increase in necrotic lesions and a loss of properly formed granulomas (Algood et al., 2005; Bean et al., 1999; Chakravarty et al., 2008; Flynn et al., 1995; Kindler et al., 1989; Roach et al., 2002). Importantly, we demonstrate that granuloma breakdown can occur independently of T cell activity. The disorganized granulomas seen in the absence of TNF signaling have been attributed to defects in the primary formation of granulomas (Flynn and Chan, 2001; Lin et al., 2007; Stenger, 2005). Our ability to monitor the sequential steps of early infection has uncovered that the loss of TNF signaling during *M. marinum* infection of zebrafish embryos leads to altered kinetics of granuloma formation, with granulomas forming more rapidly. This may be because TNF signaling may impede granuloma initiation by restricting bacterial growth early in infection. Conversely, TNF signaling deficiency causes rapid and progressive disruption of granuloma structure because of increased granuloma expansion and the accelerated necrosis of participating macrophages. Our data are consistent with the previous finding that TNF-receptor-deficient mice infected with *M. tuberculosis* formed granulomas in equal numbers to control mice when observed at early time points but that only the TNF-deficient granulomas underwent subsequent necrosis (Flynn et al., 1995). Other studies using *Mycobacterium avium* have also noted that granulomas are formed but that they rapidly disintegrate (Benini et al., 1999; Ehlers et al., 2000). Thus the deficiencies in granuloma formation noted in many studies

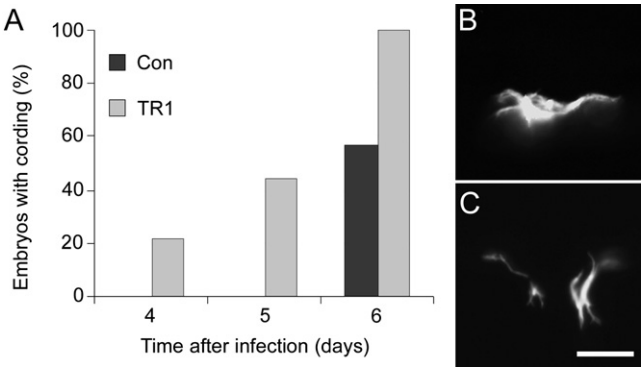

Figure 7. Increased Cording Seen in the Absence of TNF Signaling Is Not Dependent on the RD1 Virulence Locus or Granuloma Formation

(A) Control (n = 23) and TR1 morphant (n = 9) embryos were infected with 353 ± 10 ΔRD1 bacteria and scored daily for the presence of extracellular bacteria as indicated by cording and plotted as the percentage of embryos with cording. A significantly greater percentage of TR1 morphant embryos display cording versus control embryos at 5 dpi ($p < 0.01$) and 6 dpi ($p < 0.05$) as analyzed by Fisher's exact test of a contingency table. (B) and (C) show examples of cording found during infection of TR1 morphant embryos infected with ΔRD1 at 6 dpi. The scale bar represents 25 μm.

may be explained by their structural instability rather than a primary deficit in early granuloma formation (Bean et al., 1999; Kindler et al., 1989; Roach et al., 2002). Alternatively, TNF may have additional effects on granuloma structure in the context of adaptive immunity by influencing processes such as T cell trafficking and activation, and these changes may independently alter cell recruitment and structural organization in mature granulomas. This possibility is supported by recent work demonstrating that TNF is essential for recruiting T cells and retaining uninfected, but not infected, macrophages within established BCG-induced granulomas (Egen et al., 2008).

Our data suggest a model wherein TNF deficiency first leads directly to impaired macrophage defenses that result in increased intracellular bacterial burdens. The macrophage effector mechanisms downstream of TNF signaling responsible for restricting mycobacterial growth are not well characterized. iNOS activity confers resistance to mycobacterial infection in mice (Adams et al., 1997), and TNF has been found to synergize with IFN-γ to activate macrophages to produce inducible nitric oxide synthase iNOS, facilitating macrophage killing of intracellular *M. tuberculosis* (Ding et al., 1988; Flesch et al., 1994). However, our results as well as previous reports (Bean et al., 1999; Bekker et al., 2000; Ehlers et al., 1999) indicate that TNF signaling mediates macrophage microbicidal activities in the context of innate immunity that are probably not mediated by differences in nitric oxide production resulting from iNOS activity. Other known antimycobacterial mechanisms include phagolysosomal fusion (Armstrong and Hart, 1971), vitamin D-mediated bacterial killing (Liu et al., 2006) (Martineau et al., 2007), the production of reactive oxygen intermediates (Adams et al., 1997), and production and release of defensins (Miyakawa et al., 1996), small antimicrobial peptides thought to be responsible for disrupting bacterial cell-wall integrity (Menendez and Brett Finlay, 2007).

In addition to an increase in intracellular bacterial burdens in the absence of TNF signaling, there is also an accelerated necrotic death of infected macrophages both within and outside of granulomas. This increased cell death may be secondary to the accelerated increase in their bacterial burdens. The increased size of granulomas that form without TNF signaling suggests that increased bacterial burdens lead to increased numbers of heavily infected macrophages and that this increased bacterial burden ultimately leads to macrophage death and depletion. Alternatively, it is possible that the loss of TNF signaling initiates cell death via other mechanisms. The macrophage necrosis we observe may well result from the induction of the lysosomal death pathway, a caspase-independent cell-death pathway that resembles necrotic rather than apoptotic cell death (Lee et al., 2006; O'Sullivan et al., 2007). This pathway is induced by infection with *M. tuberculosis* only when bacterial burdens within macrophages are high, thus providing a potential link between the increased bacterial burdens and necrotic cell death that we observe (Lee et al., 2006; O'Sullivan et al., 2007). Although high intramacrophage bacterial burdens in the absence of TNF signaling may be sufficient to induce the lysosomal death pathway, there are multiple places where TNF signaling and its downstream effectors could potentially intersect with and influence it (Broker et al., 2005; Liu et al., 2003).

Regardless of whether increased macrophage death is a primary or secondary effect of the loss of TNF signaling, it confers a further growth advantage to the bacteria by rendering them extracellular (Clay et al., 2007). Therefore in the absence of TNF signaling, bacterial growth is enhanced at two stages: first within macrophages whose microbicidal capacity is markedly but not completely abolished and second by the death of the infected macrophages that leads to a further enhancement in bacterial replication by eliminating remaining macrophage defense mechanisms and mimicking the phenotype seen in Pu.1 morphant embryos, in which bacterial growth in the extracellular milieu is unrestricted (Clay et al., 2007). In addition, the observed acceleration of granuloma formation and death of infected macrophages both have the potential to increase net bacterial burdens by increasing cell-to-cell spread (Volkman et al., 2004) (Movie S1). Therefore our work has isolated a primary role of TNF in restricting bacteria within and to macrophages during early infection. The accelerated macrophage death that ensues further promotes bacterial growth and could also independently influence disease pathology at later stages by contributing directly to tissue destruction as well as by disrupting chemokine gradients and T cell activation, as noted during mycobacterial infection of adult animals in the absence of TNF signaling (Algood et al., 2005; Roach et al., 2002; Smith et al., 2002; Zganiacz et al., 2004).

The importance of maintaining TNF signaling during mycobacterial infection has been dramatically demonstrated by the use of anti-TNF therapeutics during treatment of chronic autoimmune disorders such as rheumatoid arthritis and Crohn's disease, which have demonstrated a particularly increased risk of tuberculosis (Gardam et al., 2003; Keane, 2005). Because of the kinetics involved when patients develop symptoms of active tuberculosis, the use of anti-TNF therapeutics has been hypothesized to result from reactivation of latent disease rather than an increased susceptibility to primary infection (Gomez-Reino et al., 2007; Keane, 2005). Notably, a number of clinical case studies of reactivated tuberculosis under these conditions have reported discrete well-formed granulomas in patient biopsies (Garcia Vidal et al., 2005; Iliopoulos et al., 2006; Lange et al., 2007; Taylor et al., 2003; Vlachaki et al., 2005; Wagner et al., 2002). Consistent with our results that a loss of TNF signaling leads to increased cell death, caseous necrosis was also found to be a major histological feature of granulomas noted in these case studies. Because the formation of caseum is a hallmark of active disease, these results suggest that the primary role for TNF signaling in human tuberculosis is also that of promoting macrophage survival. Our work has identified discrete steps of mycobacterial pathogenesis affected by this pleiotropic cytokine. Countering the specific deficits that occur during TNF blockade with downstream effectors has the potential to curtail the incidence of tuberculosis that occurs during TNF blockade. More importantly, a better understanding of TNF function may lead to a better understanding of how to enhance host defenses designed to control mycobacterial infection.

EXPERIMENTAL PROCEDURES

Animal Care and Strains

Wild-type WIK zebrafish embryos were maintained and infected with bacteria as described (Cosma et al., 2006; Davis et al., 2002; Volkman et al., 2004). Survival curves were performed by separation of embryos into 15 mL plastic petri

dishes (10–15 embryos per dish) with half-water changes twice daily, with light cycles and feeding with paramecia starting on 5 dpf.

Bacterial Strains

All bacterial strains are wild-type *Mycobacterium marinum* strain M unless otherwise indicated. Fluorescent wild-type bacteria was used and prepared as described (Davis et al., 2002). Erp mutant (Cosma et al., 2006) and ΔRD1 (Volkman et al., 2004) mutant strains were prepared as described.

Microscopy

Wide-field microscopy was performed on a Nikon E600 equipped with DIC optics, a Nikon D-FL-E fluorescence unit with 100 W Mercury lamp and MFC-1000 z-step controller (Applied Scientific Instrumentation). Objectives used included 10× Plan Fluor, 0.3 NA, 20× Plan Fluor, 0.5 NA, 40× Plan Fluor, 0.75 NA, and 60× water Fluor, 1.0 NA. Wide-field fluorescence and DIC images were captured on a CoolSnap HQ CCD camera (Photometrics) with MetaMorph 7.1 (Molecular Devices).

Three-Dimensional Image Processing

Where indicated, Z stacks were deconvolved with AutoDeblur Gold CWF, Version X1.4.1 (Media Cybernetics), with default settings for blind deconvolution.

Bacterial CFU Enumeration

CFU counts were taken as described (Clay et al., 2007) with the following changes: Embryos were dissociated in 100 μl PBS by grinding with a microtube pestles (USA Scientific). Because of the increased susceptibility of the Erp mutant bacteria to the decontamination protocol used for plating fish lysates, bacterial levels could only be examined by fluorescence microscopy; we have previously demonstrated that bacterial levels correlate with bacterial loads (Clay et al., 2007).

Morpholinos

Morpholinos were obtained from Genetools and injected at the one- to four-cell stage. Control and Pu.1 morpholinos were used as described (Clay et al., 2007). TNF receptor morpholinos were used as described (Bates et al., 2007). Morpholino controls used were wild-type WIK embryos (experiments for Figures 2B and 4 and Figure S1), Genetool's control morpholino (experiments for Figures 1,2A,3,5, and 6 and Figures S4 and S5), and the pbx mutant morpholino (Hernandez et al., 2004) (experiments for Figures S2 and S3).

In Situ Hybridization

Fluorescent in situ hybridization and TUNEL labeling was performed as described (Clay and Ramakrishnan, 2005), with *fms* probe and colorometric detection as described (Parichy et al., 2000).

Antibody Staining

Antibody staining for iNOS was performed with TSA detection as described (Clay and Ramakrishnan, 2005) with a rabbit polyclonal antibody (BD Biosciences) shown previously to crossreact with zebrafish iNOS (Shin et al., 2000).

Statistics

Student's unpaired t tests and contingency table analysis were performed with In-Stat software (Graphpad Software). Kaplan-meier analysis was performed with Prism (Graphpad Software).

SUPPLEMENTAL DATA

Supplemental Data include four figures and one movie and can be found with this article online at http://www.immunity.com/cgi/content/full/29/2/283/DC1/.

ACKNOWLEDGMENTS

We thank R. Lesley, K. Urdahl, and P. Edelstein for invaluable discussions and review of the manuscript, F. Fang and T. Richardson for advice and help with the nitric oxide studies, D. Tobin for first identifying the cording phenotype as a measure of extracellular bacterial growth in vivo, P. Edelstein for advice and help on statistical analyses of the data, M. Davis for help with video assembly, and L.Swaim and H. Wiedenhoft for managing the zebrafish facility. This work was funded by National Institutes of Health grants RO1 AI036396 and RO1 AI54503 and a Burroughs Wellcome Fund Award to L.R. H.C. was funded in part by PHS NRSA T32 GM07270 from the National Institute of General Medical Sciences. H.E.V. was funded in part by an American Heart Association predoctoral fellowship.

Received: January 17, 2008
Revised: April 29, 2008
Accepted: June 2, 2008
Published online: August 7, 2008

REFERENCES

Adams, L.B., Dinauer, M.C., Morgenstern, D.E., and Krahenbuhl, J.L. (1997). Comparison of the roles of reactive oxygen and nitrogen intermediates in the host response to Mycobacterium tuberculosis using transgenic mice. Tuber. Lung Dis. *78*, 237–246.

Algood, H.M., Lin, P.L., and Flynn, J.L. (2005). Tumor necrosis factor and chemokine interactions in the formation and maintenance of granulomas in tuberculosis. Clin. Infect. Dis. *41* (*Suppl 3*), S189–S193.

Appelberg, R., Castro, A.G., Pedrosa, J., Silva, R.A., Orme, I.M., and Minoprio, P. (1994). Role of gamma interferon and tumor necrosis factor alpha during T-cell-independent and -dependent phases of Mycobacterium avium infection. Infect. Immun. *62*, 3962–3971.

Armstrong, J.A., and Hart, P.D. (1971). Response of cultured macrophages to Mycobacterium tuberculosis, with observations on fusion of lysosomes with phagosomes. J. Exp. Med. *134*, 713–740.

Bates, J.M., Akerlund, J., Mittge, E., and Guillemin, K. (2007). Intestinal alkaline phosphatase detoxifies lipopolysaccharide and prevents inflammation in zebrafish in response to the gut microbiota. Cell Host Microbe, in press.

Bean, A.G., Roach, D.R., Briscoe, H., France, M.P., Korner, H., Sedgwick, J.D., and Britton, W.J. (1999). Structural deficiencies in granuloma formation in TNF gene-targeted mice underlie the heightened susceptibility to aerosol Mycobacterium tuberculosis infection, which is not compensated for by lymphotoxin. J. Immunol. *162*, 3504–3511.

Bekker, L.G., Moreira, A.L., Bergtold, A., Freeman, S., Ryffel, B., and Kaplan, G. (2000). Immunopathologic effects of tumor necrosis factor alpha in murine mycobacterial infection are dose dependent. Infect. Immun. *68*, 6954–6961.

Benini, J., Ehlers, E.M., and Ehlers, S. (1999). Different types of pulmonary granuloma necrosis in immunocompetent vs. TNFRp55-gene-deficient mice aerogenically infected with highly virulent Mycobacterium avium. J. Pathol. *189*, 127–137.

Berrington, W.R., and Hawn, T.R. (2007). Mycobacterium tuberculosis, macrophages, and the innate immune response: Does common variation matter? Immunol. Rev. *219*, 167–186.

Bhatt, A., Fujiwara, N., Bhatt, K., Gurcha, S.S., Kremer, L., Chen, B., Chan, J., Porcelli, S.A., Kobayashi, K., Besra, G.S., and Jacobs, W.R., Jr. (2007). Deletion of kasB in Mycobacterium tuberculosis causes loss of acid-fastness and subclinical latent tuberculosis in immunocompetent mice. Proc. Natl. Acad. Sci. USA *104*, 5157–5162.

Botha, T., and Ryffel, B. (2003). Reactivation of latent tuberculosis infection in TNF-deficient mice. J. Immunol. *171*, 3110–3118.

Broker, L.E., Kruyt, F.A., and Giaccone, G. (2005). Cell death independent of caspases: A review. Clin. Cancer Res. *11*, 3155–3162.

Chakravarty, S.D., Zhu, G., Tsai, M.C., Mohan, V.P., Marino, S., Kirschner, D.E., Huang, L., Flynn, J., and Chan, J. (2008). Tumor necrosis factor blockade in chronic murine tuberculosis enhances granulomatous inflammation and disorganizes granulomas in the lungs. Infect. Immun. *76*, 916–926.

Clay, H., Davis, J.M., Beery, D., Huttenlocher, A., Lyons, S.E., and Ramakrishnan, L. (2007). Dichotomous role of the macrophage in early mycobacterium marinum infection of the zebrafish. Cell Host Microbe *2*, 29–39.

Clay, H., and Ramakrishnan, L. (2005). Multiplex Fluorescent in situ hybridization in zebrafish embryos using tyramide signal amplification. Zebrafish *2*, 105–111.

Cosma, C.L., Klein, K., Kim, R., Beery, D., and Ramakrishnan, L. (2006). Mycobacterium marinum Erp is a virulence determinant required for cell wall integrity and intracellular survival. Infect. Immun. *74*, 3125–3133.

Cosma, C.L., Sherman, D.R., and Ramakrishnan, L. (2003). The secret lives of the pathogenic mycobacteria. Annu. Rev. Microbiol. *57*, 641–676.

Criscione, L.G., and St Clair, E.W. (2002). Tumor necrosis factor-alpha antagonists for the treatment of rheumatic diseases. Curr. Opin. Rheumatol. *14*, 204–211.

Dannenberg, A.M., Jr. (1993). Immunopathogenesis of pulmonary tuberculosis. Hosp. Pract. (Off. Ed.) *28*, 51–58.

Darzins, E., and Fahr, G. (1956). Cord-forming property, lethality and pathogenicity of Mycobacteria. Dis. Chest *30*, 642–648.

Davis, J.M., Clay, H., Lewis, J.L., Ghori, N., Herbomel, P., and Ramakrishnan, L. (2002). Real-time visualization of mycobacterium-macrophage interactions leading to initiation of granuloma formation in zebrafish embryos. Immunity *17*, 693–702.

Ding, A.H., Nathan, C.F., and Stuehr, D.J. (1988). Release of reactive nitrogen intermediates and reactive oxygen intermediates from mouse peritoneal macrophages. Comparison of activating cytokines and evidence for independent production. J. Immunol. *141*, 2407–2412.

Draper, B.W., Morcos, P.A., and Kimmel, C.B. (2001). Inhibition of zebrafish fgf8 pre-mRNA splicing with morpholino oligos: A quantifiable method for gene knockdown. Genesis *30*, 154–156.

Dubos, R.J., and Pierce, C.H. (1956). Differential characteristics in vitro and in vivo of several substrains of BCG. II. Morphologic characteristics in vitro and in vivo. Am. Rev. Tuberc. *74*, 667–682.

Egen, J.G., Rothfuchs, A.G., Feng, C.G., Winter, N., Sher, A., and Germain, R.N. (2008). Macrophage and T cell dynamics during the development and disintegration of mycobacterial granulomas. Immunity *28*, 271–284.

Ehlers, S., Benini, J., Kutsch, S., Endres, R., Rietschel, E.T., and Pfeffer, K. (1999). Fatal granuloma necrosis without exacerbated mycobacterial growth in tumor necrosis factor receptor p55 gene-deficient mice intravenously infected with Mycobacterium avium. Infect. Immun. *67*, 3571–3579.

Ehlers, S., Kutsch, S., Ehlers, E.M., Benini, J., and Pfeffer, K. (2000). Lethal granuloma disintegration in mycobacteria-infected TNFRp55−/− mice is dependent on T cells and IL-12. J. Immunol. *165*, 483–492.

Engele, M., Stossel, E., Castiglione, K., Schwerdtner, N., Wagner, M., Bolcskei, P., Rollinghoff, M., and Stenger, S. (2002). Induction of TNF in human alveolar macrophages as a potential evasion mechanism of virulent Mycobacterium tuberculosis. J. Immunol. *168*, 1328–1337.

Flesch, I.E., Hess, J.H., Oswald, I.P., and Kaufmann, S.H. (1994). Growth inhibition of Mycobacterium bovis by IFN-gamma stimulated macrophages: Regulation by endogenous tumor necrosis factor-alpha and by IL-10. Int. Immunol. *6*, 693–700.

Flesch, I.E., and Kaufmann, S.H. (1990). Activation of tuberculostatic macrophage functions by gamma interferon, interleukin-4, and tumor necrosis factor. Infect. Immun. *58*, 2675–2677.

Flynn, J.L., and Chan, J. (2001). Immunology of tuberculosis. Annu. Rev. Immunol. *19*, 93–129.

Flynn, J.L., Goldstein, M.M., Chan, J., Triebold, K.J., Pfeffer, K., Lowenstein, C.J., Schreiber, R., Mak, T.W., and Bloom, B.R. (1995). Tumor necrosis factor-alpha is required in the protective immune response against Mycobacterium tuberculosis in mice. Immunity *2*, 561–572.

Fratazzi, C., Arbeit, R.D., Carini, C., Balcewicz-Sablinska, M.K., Keane, J., Kornfeld, H., and Remold, H.G. (1999). Macrophage apoptosis in mycobacterial infections. J. Leukoc. Biol. *66*, 763–764.

Garcia Vidal, C., Rodriguez Fernandez, S., Martinez Lacasa, J., Salavert, M., Vidal, R., Rodriguez Carballeira, M., and Garau, J. (2005). Paradoxical response to antituberculous therapy in infliximab-treated patients with disseminated tuberculosis. Clin. Infect. Dis. *40*, 756–759.

Gardam, M.A., Keystone, E.C., Menzies, R., Manners, S., Skamene, E., Long, R., and Vinh, D.C. (2003). Anti-tumour necrosis factor agents and tuberculosis risk: Mechanisms of action and clinical management. Lancet Infect. Dis. *3*, 148–155.

Glickman, M.S., Cox, J.S., and Jacobs, W.R., Jr. (2000). A novel mycolic acid cyclopropane synthetase is required for cording, persistence, and virulence of Mycobacterium tuberculosis. Mol. Cell *5*, 717–727.

Gomez-Reino, J.J., Carmona, L., and Angel Descalzo, M. (2007). Risk of tuberculosis in patients treated with tumor necrosis factor antagonists due to incomplete prevention of reactivation of latent infection. Arthritis Rheum. *57*, 756–761.

Guinn, K.M., Hickey, M.J., Mathur, S.K., Zakel, K.L., Grotzke, J.E., Lewinsohn, D.M., Smith, S., and Sherman, D.R. (2004). Individual RD1-region genes are required for export of ESAT-6/CFP-10 and for virulence of Mycobacterium tuberculosis. Mol. Microbiol. *51*, 359–370.

Herbomel, P., Thisse, B., and Thisse, C. (1999). Ontogeny and behaviour of early macrophages in the zebrafish embryo. Development *126*, 3735–3745.

Herbomel, P., Thisse, B., and Thisse, C. (2001). Zebrafish early macrophages colonize cephalic mesenchyme and developing brain, retina, and epidermis through a M-CSF receptor-dependent invasive process. Dev. Biol. *238*, 274–288.

Hernandez, R.E., Rikhof, H.A., Bachmann, R., and Moens, C.B. (2004). vhnf1 integrates global RA patterning and local FGF signals to direct posterior hindbrain development in zebrafish. Development *131*, 4511–4520.

Hsu, T., Hingley-Wilson, S.M., Chen, B., Chen, M., Dai, A.Z., Morin, P.M., Marks, C.B., Padiyar, J., Goulding, C., Gingery, M., et al. (2003). The primary mechanism of attenuation of bacillus Calmette-Guerin is a loss of secreted lytic function required for invasion of lung interstitial tissue. Proc. Natl. Acad. Sci. USA *100*, 12420–12425.

Huerta, S., Goulet, E.J., Huerta-Yepez, S., and Livingston, E.H. (2007). Screening and detection of apoptosis. J. Surg. Res. *139*, 143–156.

Iliopoulos, A., Psathakis, K., Aslanidis, S., Skagias, L., and Sfikakis, P.P. (2006). Tuberculosis and granuloma formation in patients receiving anti-TNF therapy. Int. J. Tuberc. Lung Dis. *10*, 588–590.

Kaku, T., Kawamura, I., Uchiyama, R., Kurenuma, T., and Mitsuyama, M. (2007). RD1 region in mycobacterial genome is involved in the induction of necrosis in infected RAW264 cells via mitochondrial membrane damage and ATP depletion. FEMS Microbiol. Lett. *274*, 189–195.

Kaneko, H., Yamada, H., Mizuno, S., Udagawa, T., Kazumi, Y., Sekikawa, K., and Sugawara, I. (1999). Role of tumor necrosis factor-alpha in Mycobacterium-induced granuloma formation in tumor necrosis factor-alpha-deficient mice. Lab. Invest. *79*, 379–386.

Kaufmann, S.H. (2000). Is the development of a new tuberculosis vaccine possible? Nat. Med. *6*, 955–960.

Keane, J. (2005). TNF-blocking agents and tuberculosis: New drugs illuminate an old topic. Rheumatology (Oxford) *44*, 714–720.

Kindler, V., Sappino, A.P., Grau, G.E., Piguet, P.F., and Vassalli, P. (1989). The inducing role of tumor necrosis factor in the development of bactericidal granulomas during BCG infection. Cell *56*, 731–740.

Koch, R. (1882). The Aetiology of Tuberculosis (New York: National Tuberculosis Association).

Kwon, O.J. (1997). The role of nitric oxide in the immune response of tuberculosis. J. Korean Med. Sci. *12*, 481–487.

Lange, C., Hellmich, B., Ernst, M., and Ehlers, S. (2007). Rapid immunodiagnosis of tuberculosis in a woman receiving anti-TNF therapy. Nat. Clin. Pract. Rheumatol. *3*, 528–534.

Lawn, S.D., Butera, S.T., and Shinnick, T.M. (2002). Tuberculosis unleashed: The impact of human immunodeficiency virus infection on the host granulomatous response to Mycobacterium tuberculosis. Microbes Infect. *4*, 635–646.

Lee, J., Remold, H.G., Ieong, M.H., and Kornfeld, H. (2006). Macrophage apoptosis in response to high intracellular burden of Mycobacterium tuberculosis is mediated by a novel caspase-independent pathway. J. Immunol. *176*, 4267–4274.

Lin, P.L., Plessner, H.L., Voitenok, N.N., and Flynn, J.L. (2007). Tumor necrosis factor and tuberculosis. J. Investig. Dermatol. Symp. Proc. *12*, 22–25.

Liu, N., Raja, S.M., Zazzeroni, F., Metkar, S.S., Shah, R., Zhang, M., Wang, Y., Bromme, D., Russin, W.A., Lee, J.C., et al. (2003). NF-kappaB protects from the lysosomal pathway of cell death. EMBO J. *22*, 5313–5322.

Liu, P.T., Stenger, S., Li, H., Wenzel, L., Tan, B.H., Krutzik, S.R., Ochoa, M.T., Schauber, J., Wu, K., Meinken, C., et al. (2006). Toll-like receptor triggering of a vitamin D-mediated human antimicrobial response. Science *311*, 1770–1773.

Locksley, R.M., Killeen, N., and Lenardo, M.J. (2001). The TNF and TNF receptor superfamilies: Integrating mammalian biology. Cell *104*, 487–501.

Martineau, A.R., Wilkinson, K.A., Newton, S.M., Floto, R.A., Norman, A.W., Skolimowska, K., Davidson, R.N., Sorensen, O.E., Kampmann, B., Griffiths, C.J., and Wilkinson, R.J. (2007). IFN-gamma- and TNF-independent vitamin D-inducible human suppression of mycobacteria: The role of cathelicidin LL-37. J. Immunol. *178*, 7190–7198.

Menendez, A., and Brett Finlay, B. (2007). Defensins in the immunology of bacterial infections. Curr. Opin. Immunol. *19*, 385–391.

Middlebrook, G., Dubos, R.J., and Pierce, C. (1947). Virulence and morphological characteristics of mammalian tubercle bacilli. J. Exp. Med. *86*, 175–184.

Miyakawa, Y., Ratnakar, P., Rao, A.G., Costello, M.L., Mathieu-Costello, O., Lehrer, R.I., and Catanzaro, A. (1996). In vitro activity of the antimicrobial peptides human and rabbit defensins and porcine leukocyte protegrin against Mycobacterium tuberculosis. Infect. Immun. *64*, 926–932.

Mohan, V.P., Scanga, C.A., Yu, K., Scott, H.M., Tanaka, K.E., Tsang, E., Tsai, M.M., Flynn, J.L., and Chan, J. (2001). Effects of tumor necrosis factor alpha on host immune response in chronic persistent tuberculosis: Possible role for limiting pathology. Infect. Immun. *69*, 1847–1855.

O'Sullivan, M.P., O'Leary, S., Kelly, D.M., and Keane, J. (2007). A caspase-independent pathway mediates macrophage cell death in response to Mycobacterium tuberculosis infection. Infect. Immun. *75*, 1984–1993.

Pan, H., Yan, B.S., Rojas, M., Shebzukhov, Y.V., Zhou, H., Kobzik, L., Higgins, D.E., Daly, M.J., Bloom, B.R., and Kramnik, I. (2005). Ipr1 gene mediates innate immunity to tuberculosis. Nature *434*, 767–772.

Parichy, D.M., Ransom, D.G., Paw, B., Zon, L.I., and Johnson, S.L. (2000). An orthologue of the kit-related gene fms is required for development of neural crest-derived xanthophores and a subpopulation of adult melanocytes in the zebrafish, Danio rerio. Development *127*, 3031–3044.

Pressley, M.E., Phelan, P.E., 3rd, Witten, P.E., Mellon, M.T., and Kim, C.H. (2005). Pathogenesis and inflammatory response to Edwardsiella tarda infection in the zebrafish. Dev. Comp. Immunol. *29*, 501–513.

Roach, D.R., Bean, A.G., Demangel, C., France, M.P., Briscoe, H., and Britton, W.J. (2002). TNF regulates chemokine induction essential for cell recruitment, granuloma formation, and clearance of mycobacterial infection. J. Immunol. *168*, 4620–4627.

Rojo, I., de Ilarduya, O.M., Estonba, A., and Pardo, M.A. (2007). Innate immune gene expression in individual zebrafish after Listonella anguillarum inoculation. Fish Shellfish Immunol. *23*, 1285–1293.

Shin, D.H., Lim, H.S., Cho, S.K., Lee, H.Y., Lee, H.W., Lee, K.H., Chung, Y.H., Cho, S.S., Ik Cha, C., and Hwang, D.H. (2000). Immunocytochemical localization of neuronal and inducible nitric oxide synthase in the retina of zebrafish, Brachydanio rerio. Neurosci. Lett. *292*, 220–222.

Smith, S., Liggitt, D., Jeromsky, E., Tan, X., Skerrett, S.J., and Wilson, C.B. (2002). Local role for tumor necrosis factor alpha in the pulmonary inflammatory response to Mycobacterium tuberculosis infection. Infect. Immun. *70*, 2082–2089.

Stamm, L.M., Morisaki, J.H., Gao, L.Y., Jeng, R.L., McDonald, K.L., Roth, R., Takeshita, S., Heuser, J., Welch, M.D., and Brown, E.J. (2003). Mycobacterium marinum escapes from phagosomes and is propelled by actin-based motility. J. Exp. Med. *198*, 1361–1368.

Stenger, S. (2005). Immunological control of tuberculosis: Role of tumour necrosis factor and more. Ann. Rheum. Dis. *64* (*Suppl 4*), iv24–iv28.

Stinear, T.P., Seemann, T., Harrison, P.F., Jenkin, G.A., Davies, J.K., Johnson, P.D., Abdellah, Z., Arrowsmith, C., Chillingworth, T., Churcher, C., et al. (2008). Insights from the complete genome sequence of Mycobacterium marinum on the evolution of Mycobacterium tuberculosis. Genome Res. *18*, 729–741.

Swaim, L.E., Connolly, L.E., Volkman, H.E., Humbert, O., Born, D.E., and Ramakrishnan, L. (2006). Mycobacterium marinum infection of adult zebrafish causes caseating granulomatous tuberculosis and is moderated by adaptive immunity. Infect. Immun. *74*, 6108–6117.

Taylor, J.C., Orkin, R., and Lanham, J. (2003). Tuberculosis following therapy with infliximab may be refractory to antibiotic therapy. Rheumatology (Oxford) *42*, 901–902.

Tobin, D.M., and Ramakrishnan, L. (2008). Comparative pathogenesis of Mycobacterium marinum and Mycobacterium tuberculosis. Cell. Microbiol. *10*, 1027–1039.

Tosh, K., Campbell, S.J., Fielding, K., Sillah, J., Bah, B., Gustafson, P., Manneh, K., Lisse, I., Sirugo, G., Bennett, S., et al. (2006). Variants in the SP110 gene are associated with genetic susceptibility to tuberculosis in West Africa. Proc. Natl. Acad. Sci. USA *103*, 10364–10368.

Traver, D., Herbomel, P., Patton, E.E., Murphey, R.D., Yoder, J.A., Litman, G.W., Catic, A., Amemiya, C.T., Zon, L.I., and Trede, N.S. (2003). The zebrafish as a model organism to study development of the immune system. Adv. Immunol. *81*, 253–330.

Trede, N.S., Langenau, D.M., Traver, D., Look, A.T., and Zon, L.I. (2004). The use of zebrafish to understand immunity. Immunity *20*, 367–379.

Ulrichs, T., and Kaufmann, S.H. (2006). New insights into the function of granulomas in human tuberculosis. J. Pathol. *208*, 261–269.

van Crevel, R., Ottenhoff, T.H., and van der Meer, J.W. (2002). Innate immunity to Mycobacterium tuberculosis. Clin. Microbiol. Rev. *15*, 294–309.

Vassalli, P. (1992). The pathophysiology of tumor necrosis factors. Annu. Rev. Immunol. *10*, 411–452.

Vlachaki, E., Psathakis, K., Tsintiris, K., and Iliopoulos, A. (2005). Delayed response to anti-tuberculosis treatment in a patient on infliximab. Respir. Med. *99*, 648–652.

Volkman, H.E., Clay, H., Beery, D., Chang, J.C., Sherman, D.R., and Ramakrishnan, L. (2004). Tuberculous granuloma formation is enhanced by a mycobacterium virulence determinant. PLoS Biol. *2*, e367.

Wagner, T.E., Huseby, E.S., and Huseby, J.S. (2002). Exacerbation of Mycobacterium tuberculosis enteritis masquerading as Crohn's disease after treatment with a tumor necrosis factor-alpha inhibitor. Am. J. Med. *112*, 67–69.

Zganiacz, A., Santosuosso, M., Wang, J., Yang, T., Chen, L., Anzulovic, M., Alexander, S., Gicquel, B., Wan, Y., Bramson, J., et al. (2004). TNF-alpha is a critical negative regulator of type 1 immune activation during intracellular bacterial infection. J. Clin. Invest. *113*, 401–413.